Sebastian Mroz, Andriy Milenin and Henryk Dyja:

Numerical modeling of stock stability in the roll grooves during shape rolling

Stability of stock in the roll grooves depends mainly on its accurate entrance into the grooves and its support by rolling fittings. The loss of the stock stability in the grooves leads to changes of groove filling, and consequently to the appearance of product defects.
In this paper the mathematical model of the automated computer program SortRoll is used to theoretical study stock stability. The program is based on three-dimensional solution by the finite element method which allows calculation of metal flow features in the whole rolling deformation zone and accounts for stock shape and position, its temperature, velocity, rheological properties and friction condition. Regarding all those parameters allows an evaluation of stability of shape rolling in the grooves.
Sensitivity analysis of final shape and rolling stability to the stock entrance angle is fulfilled.

The processes of rolling in grooves are characterized by a spatial state of deformation and, due to their complexity, are difficult for detailed characterization. Specifically, the pattern of metal flow in particular grooves is particularly difficult to determine. In order to perform computer simulations of these processes, it is necessary to employ mathematical models that utilize the complete three-dimensional solution made by the finite-element method.

Computer modeling is the cheapest of the possible ways of process analysis and, at the same time, it provides a huge amount of information that is impossible to acquire by other methods. The purpose of carrying out computer simulations is the verification of technologies being designed for rods of different shapes and of different materials in the real technical conditions of a rolling mill, prior to their implementation.

If the axes of symmetry of strip, at the moment of its feeding to the pass, coincide with the axes of this pass and will not change their position after the strip has been bitten by the rolls and then later on in the rolling process, then there is a stable positioning of the strip in the pass. The stability of strip in the pass depends to a large extent on the accurate feed of the strip to the pass and retaining it there by the guiding gear, but conditions during strip contact with the rolls at the entrance to the roll gap, the position of the surface of initial metal and roll contact, and the geometrical proportions of pass and strip dimensions are also essential. Loss of strip stability in the pass occurs as a result of disturbance in the balance of forces on the surface of strip and roll contact, when nonsymmetrical contact surfaces relative to the rolling axis occur, caused by incorrect strip rotation by a certain angle in relation to the vertical pass symmetry axis, and pass offsetting or slanting.

From data in the literature it has been shown that strip, being fed at a certain angle to the pass, inclines toward the pass flange or top [1, 2]. The stock stability in the roll grooves depends on the groove shape, roll diameter and the factor of friction between metal and roll contact surfaces. By analyzing the proportions of geometrical dimensions in respective passes, one of the most important indices for non-equiaxial passes can be found, namely the ratio of the longitudinal axes of the pass, $a_w = B_w / H_w$, and of the strip, respectively, prior to rolling, $a_0 = h_0 / b_0$, and after rolling, $a_1 = b_1 / h_1$. The pass and strip shape indices characterize the stability of strip positioning during rolling in each pass.

Characterization of materials used for investigations

The correctness of computation using a computer program is dependent on the properties of materials used for examinations. Experiments undertaken were aimed to establish the effect of deformation parameters on the value of yield stress for the St3S steel. Chemical composition of material used for tests is given in **Table 1.**

The experimental examination of the properties of the St3S steel were carried out at the Institute of the Modeling and Automation of Plastic Working Processes of the Czestochowa University of Technology using a dilatometer–plastometer, type DIL 805A/D. Plastometric tests were performed using deformation rates of 1.0 s^{-1}, 5.5s^{-1} and 10 s^{-1} and the temperatures of plastometric tests were, respectively: 700°C, 800°C, 900°C and 1000°C. **Fig. 1** shows the results of plastometric tests in the form of flow curves for the St3S steel. Flow stress at the temperature of 800°C is lower than that at the temperature of 900°C. No monotonic changes of the flow stress as a function of temperature (Fig.1) can be explained by allotropic transformation in that range of temperature, and it agrees with [3].

In order to obtain a mathematical relationship making the value of yield stress, σ_s, dependent on deformation parameters, (ε_i, $\dot{\varepsilon}_i$, t), the results of the tests were approximated with a functional relationship described by Equation (6). The flow stress σ_s dependence on strain intensity ε_i, strain rate $\dot{\varepsilon}_i$ and temperature t for the St3S is approximated by Henzel-Spittel formula expressed as [4]:

Table 1: chemical composition of material used for tests [%]

C	Mn	Si	Cr	Ni	S	P	Cu
0.1	0.7	0.27	0.05	0.08	0.042	0.018	0.08

PhD Sebastian Mroz (Assistance Professor), *Professor D.Sc. Andrzej Milenin* (Professor), *Professor D.Sc. Henryk Dyja* (Professor), Faculty of Materials Processing Technology and Applied Physics, Czestochowa University of Technology, Czestochowa/Poland

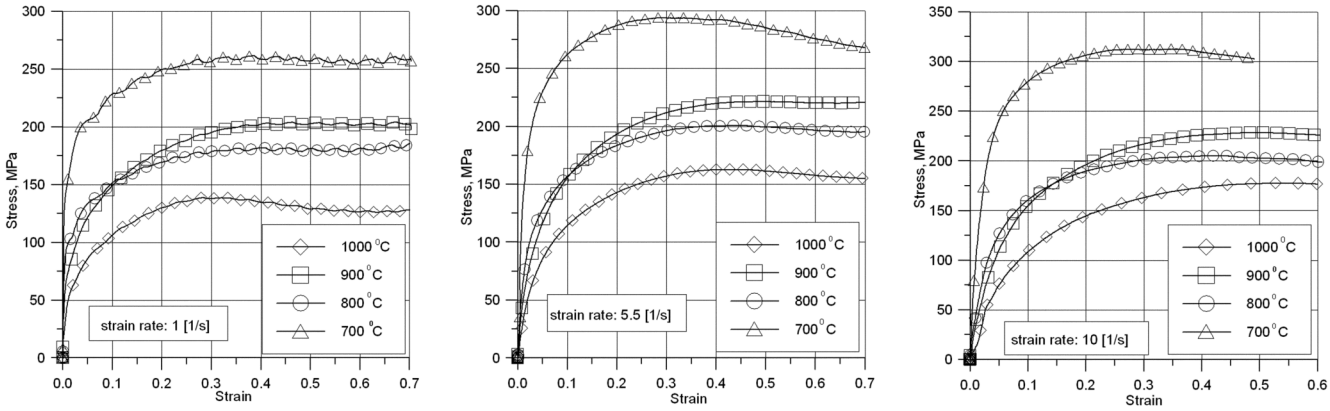

Fig. 1: work hardening curves for the St3S steel

$$\sigma_s = A_1 \cdot \varepsilon_i^{A_2} \cdot \dot{\varepsilon}_i^{A_3} \cdot \exp^{(-t \cdot A_4)} \tag{1}$$

The coefficients A_1, A_2, A_3, A_4 of the St3S steel are given in **Table 2**.

The model according to (1) does not take into account the increase of strength with increasing temperature in the tests from 800°C to 900°C. This increases the approximation error up to 24% (Table 2), but approximate results are acceptable for the purposes of this paper.

Model of the rolling process

The mathematical model for the three-dimensional metal flow of rods during the rolling in the grooves of any arbitrary shape has been developed based on principles published in references [1] and [6], by employing the finite-element method. The solution was sought for the Markov functional J [7]:

$$J = \frac{1}{2}\int_V \mu \dot{\varepsilon}_i^2 dV + \int_V \sigma \dot{\varepsilon}_0 dV - \int_S \sigma_\tau u_\tau dS \tag{2}$$

where μ – apparent metal viscosity determined from the equation:

$$\mu = \frac{\sigma_s\left(\dot{\varepsilon}_i, \varepsilon_i, t\right)}{\dot{\varepsilon}_i} \tag{3}$$

where $\sigma_s\left(\dot{\varepsilon}_i, \varepsilon_i, t\right)$ - dependence of yield stress σ_s on strain rate intensity $\dot{\varepsilon}_i$, strain intensity ε_i and temperature t; V – deformed metal volume; $\dot{\varepsilon}_0$ - relative volume change rate; σ – mean stress; u_τ – velocity of slip of metal over the tool; S – metal - tool contact surface area; σ_τ – stress of the friction at the metal-tool interface, where

$$\sigma_\tau = m\sigma_s / \sqrt{3} \tag{4}$$

m – friction factor.

Table 2: parameters of function (1) for the St3S steel

material	A_1	A_2	A_3	A_4	mean square error
St3S	1347.399	0.2197	0.0495	0.0021	0.237

Boundary conditions are taken into account by the method proposed in [8]. The essential idea of the method involves the use of a penalty function to determine the conditions of metal-tool interaction in a complex spatial configuration. Solution should be sought from the stationary condition of the modified Markov functional:

$$\begin{aligned} J = \frac{1}{2}\int_V \mu\, \dot{\varepsilon}_i^{\,2} \mathrm{dV} + \int_V \sigma \dot{\varepsilon}_0 \mathrm{dV} + \\ K_\tau \int_F \left(v_\tau\right)^2 \mathrm{dS} + K_n \int_F \left(v_n - w_n\right)^2 \mathrm{dS} \end{aligned} \tag{5}$$

$$K_\tau^{(p)} = \frac{\sigma_\tau^{(p-1)}}{u_\tau^{(p-1)}} \tag{6}$$

where: p – iteration number; $v\tau$ – metal slip velocity over the tool, v_n – metal velocity normal to the tool surface, w_n – velocity of tool surface point normal to the tool surface, $K\tau$ – the penalty coefficient accounting for the metal slip velocity over the tool (computed from (6) by the iterations), K_n – the penalty coefficient on the metal penetration into the tool.

If the penalty coefficient $K\tau$ increases, the metal slip over the contact surface is hampered. $K\tau = 0$ is related to frictionless case of deformation.

In order to include temperature in the model, the heat transfer equation was used:

$$c_{eff}\left(t\right)\rho\left(t\right)\frac{dt}{d\tau} = div\left(k\left(t\right) grad\left(t\right)\right) \tag{7}$$

where: $\rho\,(t)$– metal density, t – temperature, τ – time, $k(t)$ – heat conductivity coefficient, $c_{\mathrm{eff}}(t)$ – effective specific heat, which takes into account heat generation by deformation.

An algorithm of 3D solution of heat transfer of the bloom is built upon the sequential solutions of the plane tasks, which correspond to the movement of the cross-section through the deformation zone and air cooling zone with the rolling speed.

In order to solve the equation (7) the variation problem formulation is used in which the minimization of the following functional must be fulfilled:

$$J = \int_V \frac{1}{2}\left[k(t)\left(\frac{\partial t}{\partial x}\right)^2 + k(t)\left(\frac{\partial t}{\partial y}\right)^2 - c_{eff}(t)\rho(t)\frac{dt}{d\tau}\ t \right] dV + \int_F \frac{\alpha}{2}(t - t_\infty)^2\, dF \tag{8}$$

where: α – coefficient of heat exchange, t_∞ – temperature of environment.

Derivative of temperature with respect to time is calculated implicit by:

$$\frac{dt}{d\tau} = \frac{t_\tau - t_{\tau-\Delta\tau}}{\Delta\tau} \tag{9}$$

The model has been substantiated experimentally and a good agreement between the measured and calculated strain fields has been observed [1, 8, 9].

Results and discussion

In this study, for the theoretical examination of strip stability in the passes, experimental data (initial dimensions of square and rhomb (diamond), rhombic and square grooves, temperature and the rolling speed) were used [5]. The paper [5] reports the results of rolling of a square in the square–diamond–square pass sequence. The initial dimensions of the square stock is 50.0 x 50.0 mm in the first pass and of the rhombic stock is 74.3 x 44.0 mm. The stock temperature before the first pass is t_0 = 1204°C and before the second pass t_1 = 1131°C, the roll diameter D = 456 mm, and the rolling speed V_W = 1.5 m/s [5]. The shape and dimensions of the passes are shown in **Fig. 2**. Each pass was analyzed separately.

Within the present study, the theoretical examination of strip stability during rolling a square strip in a rhombic pass (Fig. 3a) and during rolling a rhombic strip in a square pass (Fig. 3b) was carried out. In each of the cases examined, the angle of strip twist in relation to the pass vertical axis was changed. The strip twist angle was, respectively: 0°; 5°; 10° and 15°, which is shown in **Fig. 3**. Moreover, two values of friction factor, m, were taken.

The following input data were taken for simulation:

- stock temperature of 1204°C – for the first pass (square – diamond);
- stock temperature of 1131°C – for the second pass (diamond – square);
- tool (upper and lower roll) temperature of 60°C;
- ambient temperature of 20°C;
- friction factor, m = 0.55 – variant A;
- friction factor, m = 0.85 – variant B;
- coefficient of heat exchange between the material and the tool, α = 3000 [W/Km^2];
- coefficient of heat exchange between the material and the air, α_{air} = 100 [W/Km^2].

The friction parameters were obtained by the inverse method [8] on the basis of experimental research [5]. Influence of friction in the mentioned range on the metal flow is presented in [8].

An example of FE mesh and distribution of the strain rate during rolling of square in rhombic grooves (twist angle of 15° and friction factor m = 0.85) is shown in **Fig. 4**.

After performing numerical modeling, the effect of the strip twist and the effect of friction factor, m, on rolling process parameters (such as, spread, elongation, the metal and roll contact surface area, and the rolling force).

Figure 5 illustrates the effect of the strip twist angle and

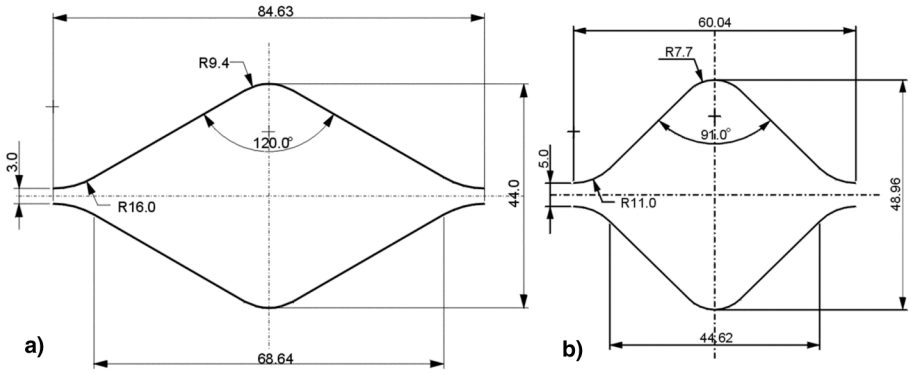

Fig. 2: shape and dimensions of grooves used during the rolling process: a) the diamond, b) the square

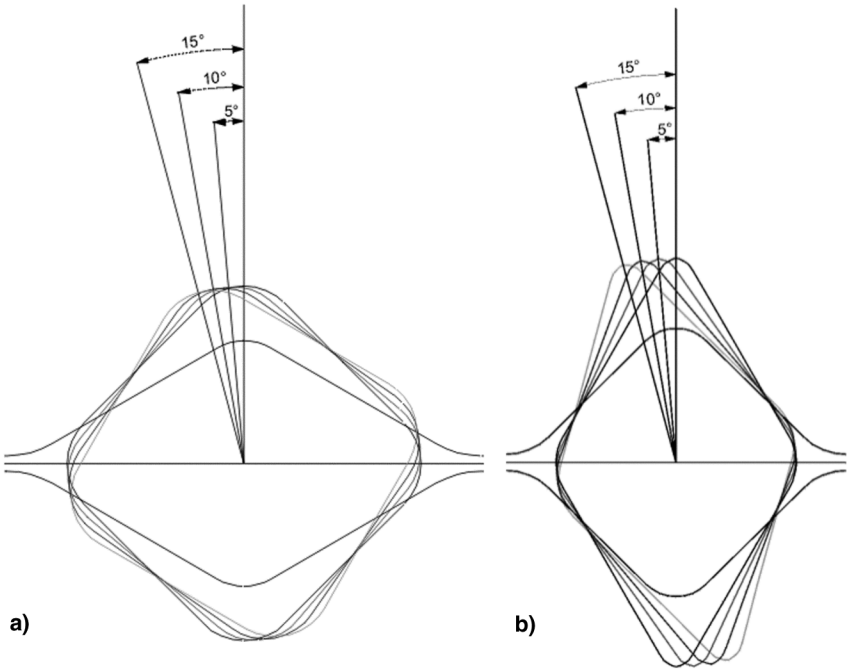

Fig. 3: scheme of initial strip positioning, for: a) square strip in the rhombic pass, and b) rhombic strip in the square pass.

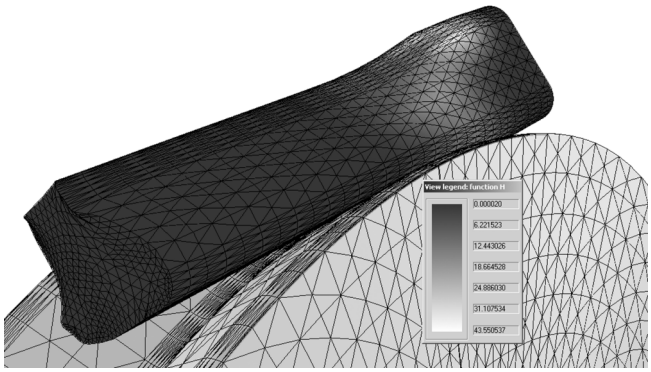

Fig. 4: view of the FE mesh and the distribution of the strain rate during rolling a square strip in a rhombic pass.

friction factor on the elongation factor. By analyzing the data in **Figs. 5a** and 5b it can be found that a change in the strip twist angle only slightly influences the elongation factor. At the same time, for the square–diamond pass (Fig. 5a), an increase in the elongation factor is found with the increase in strip twist angle, whereas for the diamond–square pass, a decrease in elongation is observed (Fig. 5b). Moreover, it can be noticed that the change of the friction factor from $m = 0.55$ to $m = 0.85$ has had a slight effect on the change of elongation.

Significant changes are noted in magnitudes of spread. **Figure 6** illustrates the effect of the strip twist angle on the spread. By analyzing the data in Fig. 6a, a substantial decrease in spread can be found, from approx. 4.7% with the correct strip feed to the pass – the twist angle of 0°, to approx. 1.5% with a strip twist angle of 15°. By analyzing the data in Fig. 6b, for the diamond–square pass, it has been found that the change of the strip twist angle from z 0° to 15° has caused an increase in spread from approximately 6% to 7.2%. The analysis of the effect of the friction factor, on the other hand, shows that, in accordance with the theory of rolling, the increase in the friction factor has resulted in an increased spread.

By making a comparison of the respective data in Figs. 5 and 6 it can be stated that either increase or decrease in elongation has caused a corresponding change in spread.

Figure 7 illustrates the effect of the strip twist angle and friction factor on the rolling force. By analyzing the data in Figs. 7a and 7b it can be noted that change in the strip twist angle only slightly influences the rolling force. Whereas, the effect observed in the square–diamond pass (Fig. 7a), is greater than for the diamond–square (Fig. 7b). Maxima can be noticed to appear for both cases. For the square–diamond, the maximum is for a strip twist angle of 10°, while for the diamond–square pass – for a strip twist angle of 5°. The behaviour of rolling force changes for the diamond–square pass is less intensive compared to the square–diamond pass. In both cases, a significant influence of the friction factor on the rolling force is noted. For simulations

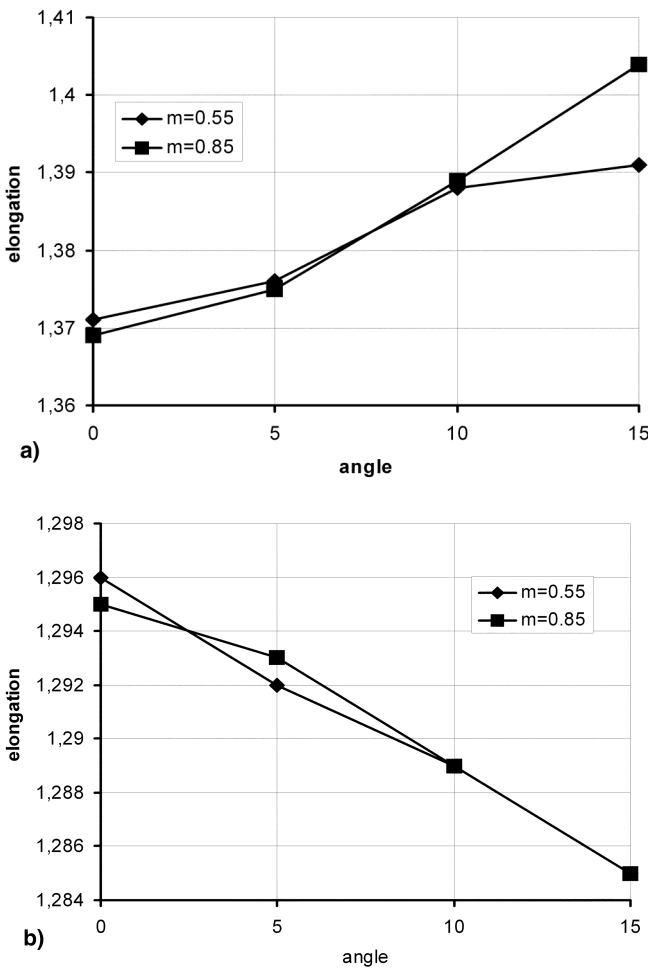

Fig. 5: influence of the strip twist angle on elongation: a) the square-diamond pass, b) the diamond-square pass

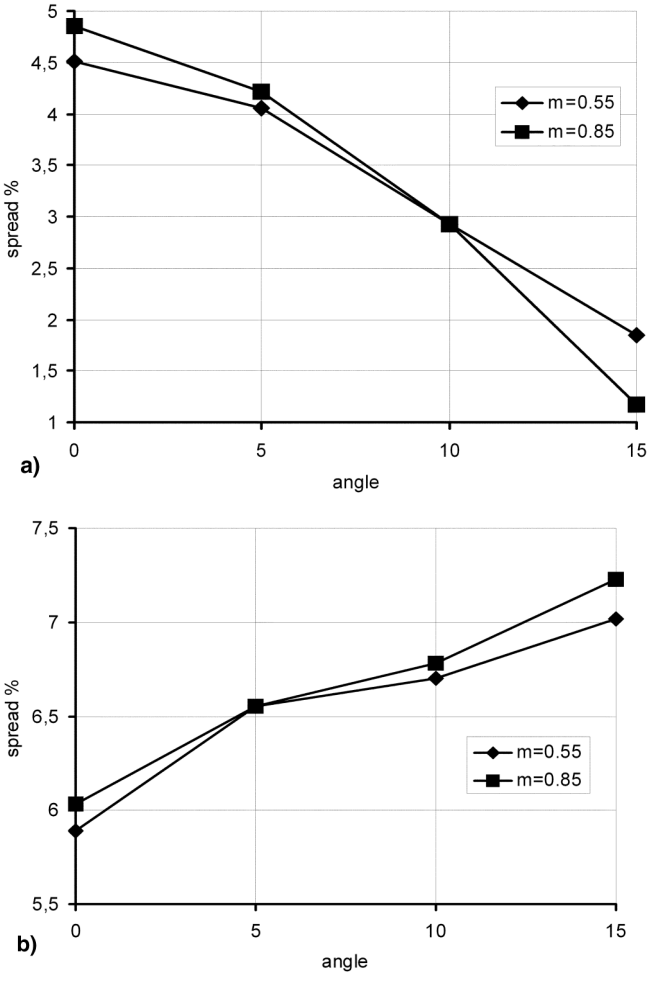

Fig. 6: influence of the strip twist angle on spread: a) the square-diamond pass, b) the diamond-square pass

carried out with a friction factor of m = 0.85, the rolling force was much higher than for simulations where the friction factor was assumed at a level of m = 0.55.

The decrease (**Fig. 7a**) or increase (**Fig. 7b**) in the rolling force after a specified strip twist angle was exceeded can be explained by the strip loosing its stability and inclination toward the pass flange. More dramatic changes were obtained for simulations, where a friction factor of m = 0.55 was used.

One of the factors influencing the rolling force, in addition to friction, is the metal and roll contact surface area. Figure 8 illustrates the effect of the strip twist angle and friction factor on the magnitude of this parameter. By analyzing the data in **Figs. 8a** and **8b**, a significant effect of the change in the strip twist angle (particularly for the square–diamond pass) on the magnitude of metal and roll contact surface area has been found. In the both cases (the square–diamond and diamond–square), maxima of this quantity can be noticed at the strip twist angle equal to 5°. These maxima coincide with those occurring with the change in the rolling force (in particular, for the diamond–square pass). Moreover, in both cases, the metal and roll contact surface area was greater for computer simulations performed with a friction factor of m = 0.85. Larger values of the metal and roll contact surface area correspond to the spread which, for simulations using a friction factor of m = 0.85, was greater.

Conclusions

- The investigation carried out enables the following observations to be made and conclusions to be drawn:
- the developed computer program SortRoll enables a comprehensive analysis of the shaped-pass rolling process;
- the shapes and dimensions of strip cross-sections and rolling force values obtained as a result of simulation allow a correction of a technology developed at the design stage, without any costs associated with experiments;
- change in the angle of strip twist relative to the vertical pass axis significantly influences the obtained geometrical and force parameters of the rolling process, irrespective of the pass arrangement;
- a particularly significant effect of the strip twist angle observed was on the change in widening – incorrect feeding of the strip to the pass may result in the pass being either overfilled or incompletely filled;
- loss of stability by the strip results in a change in the values of the rolling force and metal and roll contact surface area.

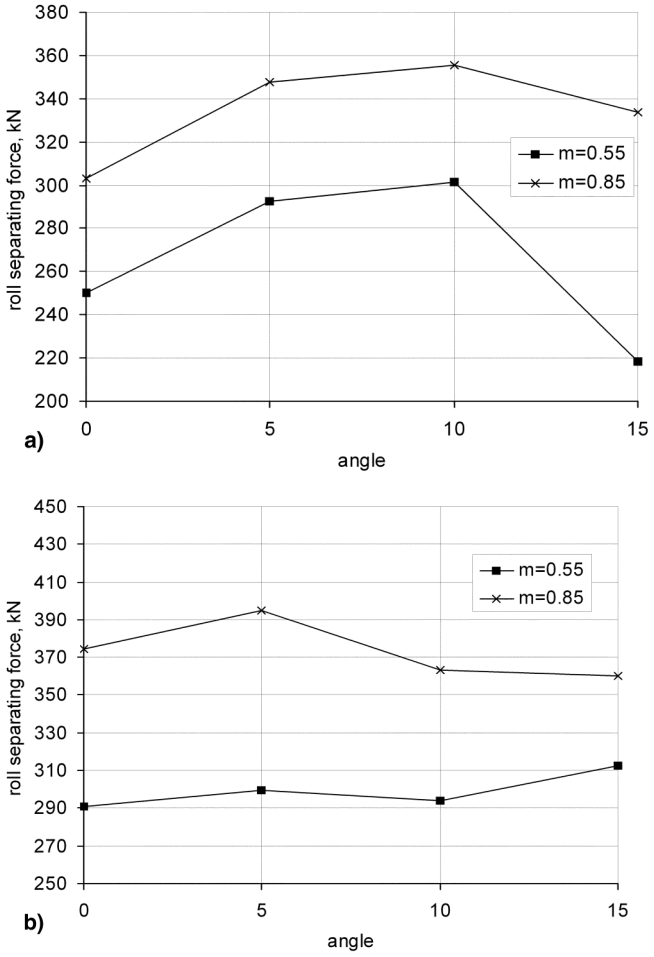

Fig. 7: influence of the strip twist angle on the roll separating force: a) the square-diamond pass, b) the diamond-square pass

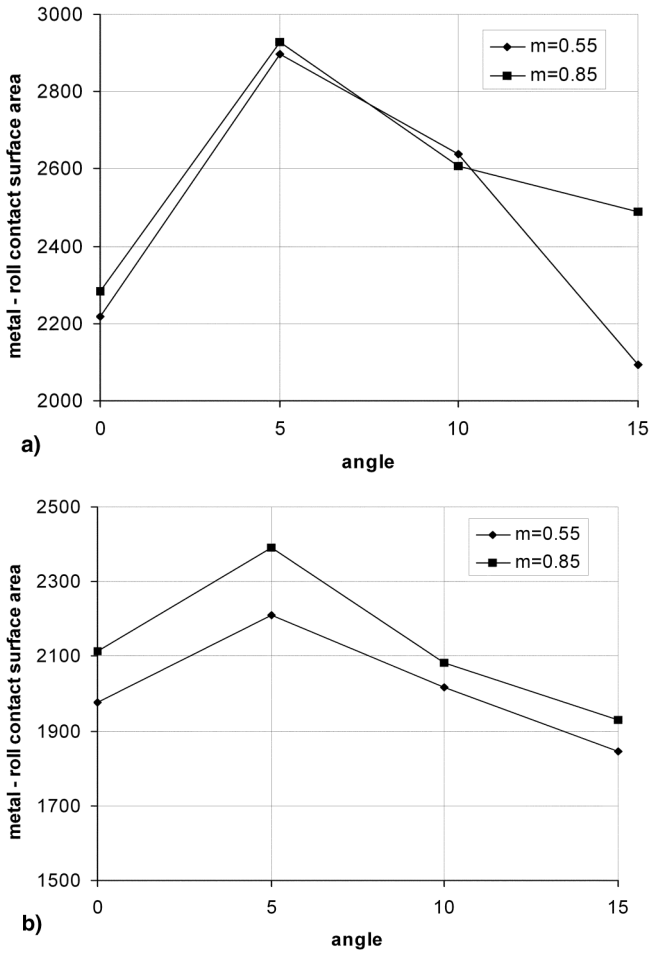

Fig. 8: influence of the strip twist angle on the metal - roll contact surface area: a) the square-diamond pass, b) the diamond-square pass

References

[1] Danchenko V., Dyja H., Lesik L., Mashkin L., Milenin A.: Technologia i modelowanie procesów walcowania w wykrojach, Seria: Metalurgia Nr 28, Częstochowa 2002 (in Polish).

[2] Smirnov V. K., Shilov N.A., Inatovich Yu.V.: Kalibrovka prokatnykh valkov, Metalurgija, Moskva, 1987 (in Russian).

[3] Nowakowski A., Kuźmiński Z.: Hutnik-Wiadomości Hutnicze, Vol. 63 (1996), p. 243/246 (in Polish).

[4] Henzel, T. Spittel.: Rasciet energosilovykh parametrov v processakh obrobotki metallov davlenijem, Metalurgija, Moskva, 1982 (in Russian).

[5] Coukhar G.: Silovyje vozdejstvija pri prokatke v vytjazhnykh kalibtakh, Metalurgija, Moskva, 1963 (in Russian).

[6] Milenin A., Dyja H., Lesik L., Mróz S.: Prokatnoje Proizvodstvo, Vol. 12 (2001), p. 8/13 (in Russian).

[7] Markov A.: O variacionnykh principakh w teorii plastichnosti, Prikladnaja matematika i mekhanika, Vol. 11 (1947), p. 333/350 (in Russian).

[8] Dyja H., Lesik L., Milenin A., Korsun P.: Hutnik-Wiadomosci Hutnicze, Vol. 69 (2002), p. 76/79.

[9] Mróz S., Milenin A., Szota P., Kawałek A.: Wykorzystanie metody odwrotnej do wyznaczania czynnika tarcia podczas numerycznego modelowania procesu walcowania aluminiowych prętów, Nowe Technologie i Osiągnięcia w Metalurgii i Inżynierii Materiałowej, Seria: Metalurgia Nr 31, Częstochowa, 2003, p. 248/251 (in Polish).